



Land-use change may exacerbate climate change impacts on water resources in the Ganges basin

Gina Tsarouchi^{1,2,3} and Wouter Buytaert^{1,2}

¹Department of Civil and Environmental Engineering, Imperial College London, London, UK

²Grantham Institute for Climate Change and the Environment, Imperial College London, London, UK

³HR Wallingford, Howbery Park, Wallingford, Oxfordshire OX10 8BA, UK

Correspondence to: Gina Tsarouchi (g.tsarouchi@hrwallingford.com)

 **Abstract.** Quantifying how land-use change and climate change affect water resources is a challenge in hydrological science. The Upper Ganges (UG) river basin in northern India experiences monsoon flooding almost every year. Studies have shown evidence of strong coupling between the land surface (soil moisture) and atmosphere (precipitation) in northern India, which means that regional climate variations and changes in land use/cover could influence the temporal dynamics of land-atmosphere interactions.

This work aims to quantify how future projections of land-use and climate change are affecting the hydrological response of the UG river basin. Two different sets of modelling experiments were run using the JULES Land Surface Model and covering the period 2000-2035: In the first set, climate change is taken into account, as JULES was driven by the CMIP5 (Coupled Model Intercomparison Project Phase 5) outputs of 21 models, under two Representative Concentration Pathways (RCP4.5 & RCP8.5), whilst land use was kept constant at year 2010. In the second set, both climate change and land-use change were taken into consideration, as apart from the CMIP5 model outputs, JULES was also forced with a time-series of 15 future land-use scenarios, based on Landsat satellite imagery and Markov chain simulation. Variations in hydrological variables (stream flow, evapotranspiration and soil moisture) are calculated during the simulation period.

Significant changes in the near-future (years 2030-2035) hydrologic fluxes arise under future land-cover and climate change scenarios pointing towards a severe increase in high extremes of flow: the multi-model mean of the 95th percentile of streamflow [Q_5] is projected to increase by 63% under the combined land-use and climate change high emissions scenario [RCP8.5]. The changes in all examined hydrological components are greater in the combined land-use and climate change experiment.

Results are further presented in a water resources context, aiming to address potential implications of climate change from a water-demand perspective, highlighting that  demand thresholds in the UG region are projected to be exceeded in the future winter months (Dec-Feb).



1 Introduction

Over recent decades, the Indian subcontinent has undergone some of the largest environmental changes in human history. India's green revolution of widespread implementation of irrigation, application of fertilizer and other modern farming practices, besides the ubiquitous benefits, has resulted 30 in large-scale changes in land cover and a significant increase in the exploitation of water resources,  including the vast groundwater aquifers of the Gangetic plains. From 1960 to 1999, irrigation from tube wells and other wells grew by more than 400% and currently supplies well over half of the country's irrigated area (Scott, 2009). At the same time, groundwater provides 50–80% of domestic water demand (Kumar et al., 2005). Large groundwater irrigated areas increased by 187% from 35 1970 to 1999 (Zaisheng et al., 2006). These changes have put severe pressure on water resources, a pressure that is exacerbated further since the increasing demand for better diet led farmers to mainly plant high-water intensity crops such as wheat, rice and sugarcane (Kaushal and Kansal, 2011). At  the same time, groundwater levels show a steady decline (Rodell et al., 2009). The pressure on water 40 resources is expected to further increase in the near future: for example, by 2030, India's urban population is expected to rise from 286 million (in 2001) to 575 million (Tehnunen and Saavala, 2012). The country eyes double-digit economic growth, whilst the Ganges basin is the most densely populated river basin in the world, with an average population density of 520 persons/km². Between 1991 and 2001, the urban population of India increased by 32%, and this trend is likely to continue, making the study area subject to rapid land-cover changes (O'Keeffe et al., 2012). According to the 45 2011 Census (Office of the Registrar General & Census Commissioner, India, 2011), the population of India has increased by more than 181 million from 2001 to 2011, reaching 1.21 billion. Population density in Uttar Pradesh (which covers large part of our study area) has increased by more than 100% from 1971 to 2001, leading to a sharp increase in water demand (Kaushal and Kansal, 2011). Especially during dry periods outside of the summer monsoon season, users of water resources are 50 reliant upon the canals to maintain the required flow levels and sustain riverine ecology.

The Indian monsoon supplies more than 80% of India's total annual rainfall between June and September (Turner and Annamalai, 2012). The country's population depends largely on the summer monsoon rainfall for food and energy production, agricultural activities and industrial development.

 55 Since this study is interested in large-scale surface water - climate fluxes and feedbacks, the mountainous headwaters in the north of the basin are not taken into consideration. Although climate change impacts on glaciers and snow melt are of great concern, they are an intensive field of research, but have only limited impact on the water resources of the lower plains (Immerzeel et al., 2010). The large downstream monsoon-dominated system of the Ganges river basin, in combination with limited upstream precipitation and small glaciers are the reasons for this minor contribution of 60 snow and glacier water to the Ganges (Immerzeel et al., 2010).

Countrywide evidence, supported by localised studies, already suggests a decrease in frequency of light-to-moderate rainfall events and increases in heavy rainfall events, specifically in the central



and north-east region of India, since the early 1950s (Dash et al., 2009). The CMIP5 (Coupled Model Intercomparison Project Phase 5) model projections for the end of the 21st century suggest 65 an intensification of heavy precipitation events over India under RCP8.5, the "business-as-usual" scenario (Scoccimarro et al., 2013). The average summer monsoon rainfall over India is projected to increase by around 5-10% (Turner, 2013). According to these projections, precipitation intensity seems to increase more than mean precipitation under a warmer climate (Scoccimarro et al., 2013; Meehl et al., 2005), physically consistent with the greater moisture-holding capacity of warmer 70 air and leading to more intense rainfall when it does occur (Turner and Annamalai, 2012). More rainfall would increase water availability on the long term, but the potential for larger interannual and intraseasonal variability in summer rainfall could also be associated with more frequent/severe flood and drought events. The spatial patterns of these changes vary from model to model, making it difficult to project how rainfall might change within India (Turner and Slingo, 2009).
75 Over recent years, extreme weather events in South Asia, such as the July 2002 drought over India (Bhat, 2006), the Pakistan floods of July-August 2010 and the north India floods of June 2013, have claimed thousands of lives (Lau and Kim, 2011; Kala, 2014). According to Singh et al. (2014), anthropogenic climate change has increased the likelihood of extreme rainfall such as the June 2013 80 event over northern India, which along with poor environmental management, the lack of preparedness by the state and poorly planned construction and development (Kala, 2014) worsened the effects of flooding (>5800 deaths, Singh et al., 2014). In a recent report, the World Bank states that an extremely wet Indian summer monsoon, which currently occurs once every 100 years, is projected to occur once every 10 years by the end of this century (World Bank, 2013). Several other studies, including the IPCC's Fifth Assessment Report (Intergovernmental Panel on Climate Change (AR5), 85 IPCC, 2014), have linked climate change to extreme weather events over South Asia.

Future climate change and particularly the reliance of water resources on the highly erratic precipitation patterns of the summer monsoon, pose significant risks to water supply. Any change in the summer monsoon's timing, intensity and duration, affected by increases in greenhouse gas concentrations could be detrimental to water supply. Given the rapid increase in population in the region 90 and the need to improve water and food security, it is essential to understand how the climate will change in the future and how its change will impact humans and the environment.

The CMIP5 projections are likely to provide unreliable estimates of the mean values and daily variations of precipitation due to **current limitations of the General Circulation Models** (GCMs; Raty et al., 2014). Besides, GCMs were not built for the application of hydrological impact studies. 95 The runoff generation mechanism in GCMs is based on a simplistic representation of the hydrological cycle, and several studies have shown that hydrological models driven directly by GCM model outputs do not perform well (Fowler et al., 2007). To diminish the impacts of GCM biases, several techniques that adjust the climate projections and transform coarse resolution GCM outputs into finer scale products suitable for hydrological applications have been developed over recent years and



100 plenty of studies have revised and evaluated these techniques ((Fowler et al., 2007; Maraun et al.,
101 ; Teutschbein and Seibert, 2012; Raisanen and Raty, 2013; Raty et al., 2014)). In this study, the
102 delta-change method was applied on CMIP5 model outputs and observations to generate future cli-
103 mate scenarios, which where then used to run JULES and quantify the impact of climate change on
104 the hydrology of the UG river basin. Further, the combined impact of climate change and land-use
105 change is examined by using (along with the delta-change transformed observations) a time-series
106 of 15 future land-use scenarios, based on Landsat satellite imagery and Markov chain analysis (see
107 Section 3). The modeling period up to 2035 was selected as the most relevant for current water
108 resources management decisions. The entire set of available daily CMIP5 model outputs under the
109 historical, RCP4.5 and RCP8.5 experiments was used to cover the range of plausible uncertainty.
110 nderstanding and monitoring the hydrologic response of watersheds to land-use and climate
111 ange is an important element of water resource planning and management. The following hy-
112 pothesis is driving this research: "*The combined impacts of land-use and climate change will be
113 greater than the impacts posed by land-use change and climate change individually, on hydrological
114 components*". The quantification of land-use and climate change impacts on hydrological fluxes is
115 a challenge in hydrological science and especially in the data sparse tropical regions. Many studies
116 focus on climate change impacts only and others focus on land-use change impacts only. However,
117 here are just a few studies that consider the combined effects of climate and land-use change by
118 quantitatively integrating both. In this study, those relative impacts are investigated by analysing
119 annual variations of hydrological components (stream flow, evapotranspiration and soil moisture),
120 under different land-use and climate change scenarios.

The rest of this paper is structured as follows. After describing the study area and the data used in
121 Section 2, we ess the methods applied in Section 3, present the results derived in Section 4, and
122 then discuss our findings in Section 5, before concluding in Section 6. Two appendices included at
123 the end of the paper provide additional material on: (A) The CMIP5 model outputs analysis, and (B)
124 The Hydrological future projections.

2 Data, modeling tools and study area

2.1 Study domain: the Upper Ganges basin

The study area corresponds to the main upper branch of Ganges and covers an area of 87,000 km².
The domain is located in northern India between longitudes 77°E to 81°E and latitudes 25°N to
130 32°N. Elevation ranges from 7400 m in the Himalayan mountain peaks to 90 m in the plains (Fig. 1).
The UG basin lies in the states of Uttarakhand and Uttar Pradesh and the main physical subdivisions
of the area are the northern mountainous regions (Himalayan foothills) and the Gangetic plains.
In the upstream mountainous regions where the river originates, hydro-power is the main focus of
development with mega and micro projects either already operating or currently under construction



135 (Bharati et al., 2011). When the river reaches the plains, it becomes subject to vast irrigation demands
as more than 410 million people are depending on it to cover their daily needs (Vergheze, 1993).

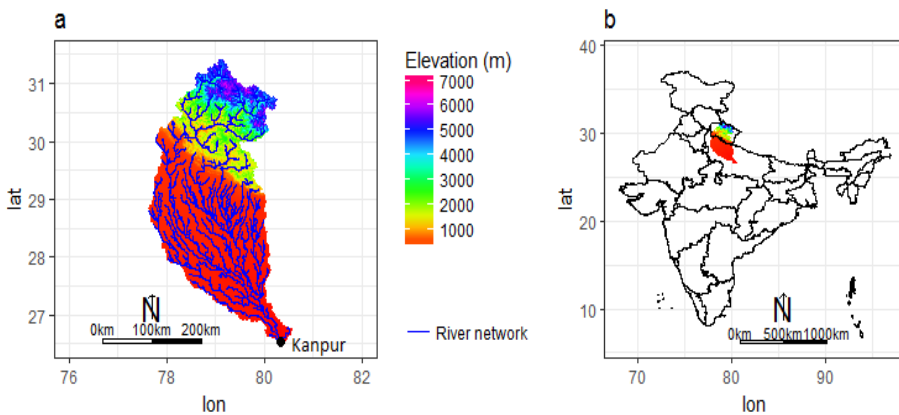


Figure 1. Location map of the study area in north India and a Digital Elevation Model (DEM) of the UG basin showing the ranges of the elevations (m altitude). Kanpur barrage was used as the outlet point.

As shown in Fig. 2, areas in the north of the UG basin (Himalayas) are either barren or covered by snow. The central and northern parts of the catchment are dominated by forests (20% of the total catchment area). Around 60% of the basin is occupied by agriculture (main crop types include wheat, 140 rice, maize, sugarcane, bajra and potato). Most of the urban and agricultural areas in the basin are located towards the south, in the plains of the UG basin.

The annual average rainfall in the UG basin ranges between approximately 610 mm and 1810 mm (Fig. 3). The main source of rainfall is the south-west monsoon, which occurs at this location from July to late September, providing more than 80% of the total annual precipitation (Turner and Anna-145 malai, 2012). The runoff regime in the UG basin is rain-dominated, due to the monsoon-dominated precipitation regime, and the maximum discharge of the river occurs during the monsoon period (Lutz et al., 2014). However, the fluctuation between monsoon flows and dry period flows is very high and that means that large areas are subjected to floods and/or droughts every year (Jain et al., 2007), resulting in significant loss of life and property (e.g. recent northern India floods in Uttarak-150 hand, June 2013).

2.2 The JULES Land Surface Model

In this study we use the Joint UK Land Environment Simulator (JULES, version 3.4) Land Surface Model (LSM) (Best et al., 2011) in order to investigate the impact of land-use change and climate change in hydrological fluxes of the UG river basin. We drive the model with statistically downscaled

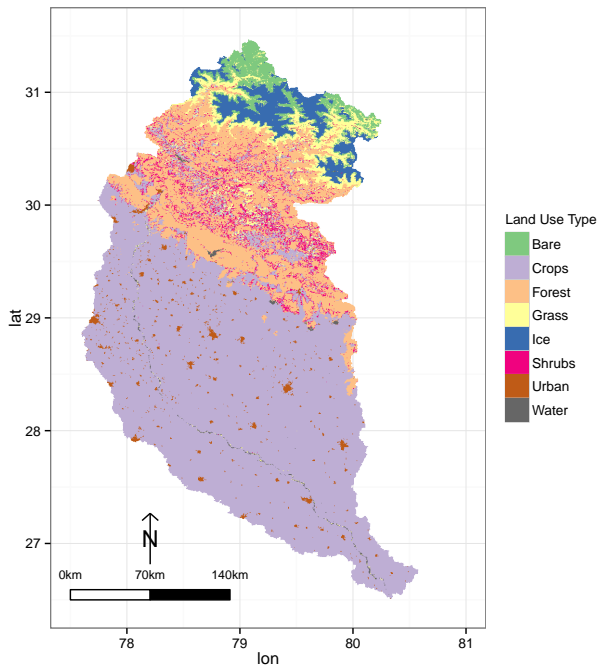


 **Figure 2.** Land-cover map of the UG basin, for year 2010, as developed by Tsarouchi et al. (2014). Landsat 7 LTM+ images, for October 2010 were acquired from the US Geological Survey Global Visualization Viewer. The images were co-registered to the UTM projection zone 44N, WGS 1984 datum and corrected for radiometric and atmospheric effects. They were subsequently classified using a Maximum Likelihood classifier method with pixel training data sets, resulting into a land cover map of eight different classes. For more information see Tsarouchi et al. (2014).

155 future climate projections from the CMIP5 multi-model database and a series of future land-use scenarios, based on Landsat satellite imagery and Markov chain analysis.

JULES was developed by the UK Met Office and is based on MOSES (Met Office Surface Exchange System), the LSM used in the Unified Model of the UK Met Office. It is a combined process-based distributed/lumped parameter model that simulates the exchange of energy, water, and carbon 160 fluxes between land surface and the atmosphere. The input meteorological data requirements are time-series of incoming short-wave and long-wave radiation, temperature, specific humidity, wind speed, and surface pressure. These are used in a full energy balance equation that includes components of radiation, sensible heat, latent heat, canopy heat, and ground surface heat.

The model partitions precipitation into canopy interception and throughfall. In the default runoff 165 scheme, surface runoff is generated based on Hortonian infiltration. Surface heterogeneity within

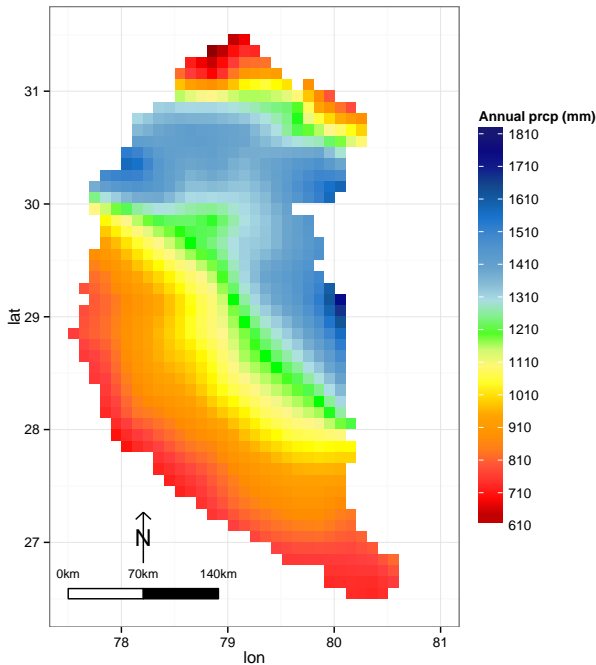


 **Figure 3.** Annual average precipitation distribution in the study area, based on TRMM 3B42v7A satellite product (years 1998–2011).

JULES is represented by the tile approach (Essery et al., 2003). The surface of each grid-box comprises fractions of 9 different land cover types; five vegetated - Plant Functional Types (PFTs): broad-leaf trees, needle-leaf trees, C_3 grasses, C_4 grasses and shrubs, and four non-vegetated: urban, water, bare soils and ice. For each surface type of the grid-box, the energy balance is solved, and a weighted average is calculated from the individual surface fluxes for each grid-box. In the subsurface, the soil column is divided into 4 layers, which have a thickness of 0.1m, 0.25m, 0.65m, and 2m respectively, going from the top to the bottom. The Darcy-Richards equation (Richards, 1931) is solved using a finite difference approximation, to calculate water movement through the soil. Subsurface runoff is represented by a free drainage from the deepest soil layer. The soil water retention characteristics (relationship between volumetric water content and soil suction) and the relationship between volumetric water content and hydraulic conductivity follow the relationships of van Genuchten (1980). For a more detailed description of the model see  Bot et al. (2011).

JULES was run in a 0.1° longitude $\times 0.1^\circ$ latitude grid resolution, for the period 2000–2035. For each grid point, the full set of input data (model parameters, time-series of meteorological data, land-use and soil map) were prescribed. Before each run of the model, a spin-up run is performed,



to initialise the internal states. For the parametrisation of plant functional types and non-vegetated tiles, [the default parameters](#) described by Best et al. (2011) and given in [Tables 5 & 6](#), were used.

2.3 [Use climate projection data from CMIP5](#)

GCM outputs from 21 models of the CMIP5 multi-model database were obtained through the UK
185 Centre for Environmental Data Analysis (CEDA). All meteorological variables required by JULES
(i.e. time-series of incoming short-wave and long-wave radiation, temperature, specific humidity,
wind speed, and surface pressure) were acquired from the historical, RCP4.5 and RCP8.5 experiments
190 of 21 CMIP5 models shown in Table 1 (those are the models that had the required daily data
available in all three experiments). RCP4.5 and RCP8.5 were chosen because they correspond to
contrasting future greenhouse gas emissions scenarios: RCP4.5 represents a "middle-of-the-road"
195 scenario, where the projected change in global mean surface air temperature for the late 21st century
(2081-2100) relative to the reference period of 1986–2005 is 1.8°C; RCP8.5 represents a "business-
as-usual" scenario of future emissions, where the projected change in global mean surface air tem-
perature for the late 21st century relative to the reference period of 1986–2005 is 3.7°C (IPCC,
2013).

To run JULES, we used CMIP5 model outputs covering the years 2000-2005 from the historical
experiment, whilst from the RCP4.5 and RCP8.5 experiments we used model outputs covering the
years 2006-2035.

2.4 **Scenarios of future land-use change**

200 For the future scenarios of land-use change, 15 maps for years up to 2035 were developed in
Tsarouchi et al. (2014), based on Landsat satellite imagery and Markov chain analysis. Under the
assumption that the drivers that caused land-use changes in recent years (2000-2010), will remain
the same in the nearby future (years up to 2035), 15 transition probability matrices indicating tran-
sition potentials from one land-use type to another were generated. These 15 transition matrices
205 are based on historic land-use transitions that occurred during the period from 2000 to 2010, where 6
land-use maps were available (one map every two years). The 15 matrices describe all possible land
use transition combinations of the years 2000, 2002, 2004, 2006, 2008, and 2010 (e.g. 2000-2002,
2000-2004, 2000-2006, etc.). The trends in different matrices vary and this is also reflected in the
future projections (i.e. they are not exactly the same).
210 Figure 4 highlights the spread of these 15 future scenarios for the year 2035 and how their land-
cover proportions compare to the historic year 2010. The variations between the different scenarios
are not large and the main trends of change identified are forest growth, urbanisation, and on the
other hand loss of bare soil, grasslands and shrubs. For a more detailed description of the method
used to generate the future land-use scenarios see Tsarouchi et al. (2014).



 **Table 1.** CMIP5 model output used and data resolution

Model	Centre	Spatial Resolution (Lon x Lat)	Country
ACCESS1-0	CSIRO-BOM	1.88°x 1.25°	Australia
ACCESS1-3	CSIRO-BOM	1.88°x 1.25°	Australia
BCC-CSM1-1-M	BCC	1.13°x 1.13°	China
BNU-ESM	BNU	2.81°x 2.81°	China
CanESM2	CCCma	2.81°x 2.81°	Canada
CNRM-CM5	CNRM-CERFACS	1.41°x 1.41°	France
CSIRO-MK3-6-0	CSIRO-QCCCE	1.88°x 1.88°	Australia
INM-CM4	INM	2.00°x 1.50°	Russia
IPSL-CM5A-LR	IPSL	3.75°x 1.88°	France
IPSL-CM5A-MR	IPSL	2.50°x 1.26°	France
IPSL-CM5B-LR	IPSL	3.75°x 1.88°	France
MIROC4h	MIROC	0.56°x 0.56°	Japan
MIROC5	MIROC	1.41°x 1.41°	Japan
MIROC-ESM	MIROC	2.81°x 2.81°	Japan
MIROC-ESM-CHEM	MIROC	2.81°x 2.81°	Japan
HadGEM2-CC	MOHC	1.88°x 1.25°	UK
HadGEM2-ES	MOHC	1.88°x 1.25°	UK
MRI-CGCM3	MRI	1.13°x 1.13°	Japan
GFDL-CM3	NOAA-GFDL	2.50°x 2.00°	US
GFDL-ESM2G	NOAA-GFDL	2.50°x 2.00°	US
GFDL-ESM2M	NOAA-GFDL	2.50°x 2.00°	US

215 The CMIP5 model outputs, together with the future land-use change maps were used to run JULES
 in a series of experiments, further described in Section 3.

2.5 Water demand data

Aiming to place our results in a future water resources context (focusing on the period 2030-2035),
 we use water demand data from a recent study by Sapkota et al. (2013). The mean monthly water
 220 demands shown in Fig.4 of Sapkota et al. (2013) are used in combination with future projections of
 changes in India's water demands, as presented in the study by Amarasinghe et al. (2007). The latter
 study suggests an expected 8% increase in surface water demand for irrigation, 130% increase in
 surface water demand for domestic usage and 152% increase in surface water demand for industrial
 usage, by 2030 under a business as usual scenario, which is mainly extrapolating trends of recent
 225 years (calculations after linearly interpolating results presented for years 2025 and 2050).

3 Methods

 Previously mentioned, the CMIP5 precipitation projections are likely to provide unreliable estimates of changes to the mean values and daily variance of precipitation due to inherent limitations

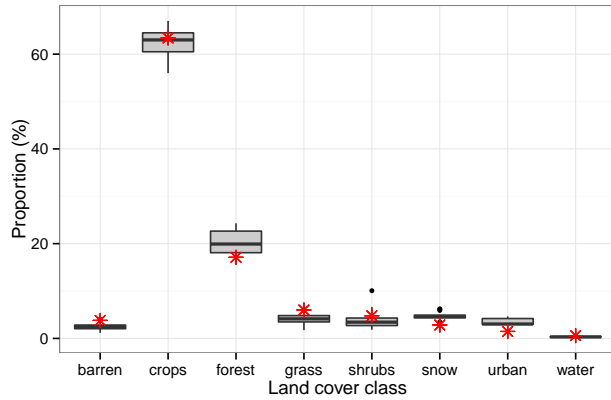


 **Figure 4.** Box plots indicating the spread of different land uses for year 2035, amongst the 15 land-use scenarios developed by applying Markov chain analysis in Tsarouchi et al. (2014). Red stars illustrate the actual land-cover proportions of year 2010, as derived from the Landsat classifications. The middle bar of each box shows the median, while the bottom and top of the box bars show the 25th and 75th percentiles (or first and third quartiles), respectively. The upper and lower whiskers extend to the highest and lowest values that are within 1.5 × IQR of the box's top and bottom bars, where IQR is the inter-quartile range. Dots show outliers.

of the GCMs (Raty et al., 2014). Biases have already been identified in simulating the present-day observed Indian summer monsoon climatologies (Sengupta and Rajeevan, 2013). Further, Lutz et al. (2014) found large uncertainties and variations between the annually averaged and seasonal precipitation projections over the UG basin. In this study, to avoid the issue of GCM biases and smoothing in the coarse-resolution time series, we applied the delta-change method to observed meteorological datasets. This is a relatively simple approach, broadly used for transforming coarse resolution GCM outputs into finer scale products suitable for hydrological applications. It calculates the change in time between the control and future simulations of a variable and applies this change in the baseline (observed) climate by simply adding or scaling the mean climatic change factor (CF) to each day (Fowler et al., 2007). This change is relative change for fluxes exchanged between the atmosphere and surface in order to avoid negative values, and absolute change for state meteorological variables.

So, for precipitation, radiation and wind speed the monthly CF is calculated as:

$$CF = \frac{\bar{V}_{fut}}{\bar{V}_{hist}} \quad (1)$$

Where \bar{V} the monthly climatological mean for a given flux variable. For temperature, pressure, and specific humidity, which are state variables, the CF is calculated as:

$$CF = \bar{V}_{fut} - \bar{V}_{hist} \quad (2)$$



However, this approach has a number of limitations: a) It assumes a constant delta for each month, as it suggests that relative change is better simulated than absolute values; b) It assumes a constant spatial pattern of the climatic variable and ignores changes in variability, as the calculated CFs only scale the mean, max and min values; c) There is no change in the temporal sequence of wet/dry days (Fowler et al., 2007).

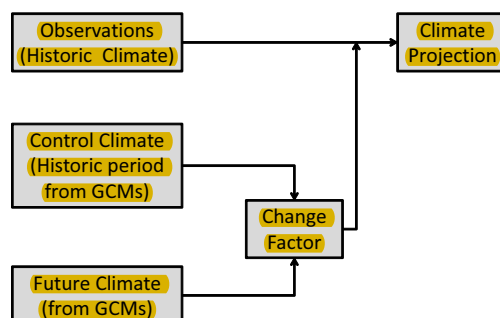


Figure 5. Flow chart of Delta Change method.

250 As baseline (observed) climate, we used for precipitation the Tropical Rainfall Measuring Mission (TRMM) Multi-satellite Precipitation Analysis (TMPA) product, version 7, (Huffman et al., 2007; Huffman and Bolvin, 2013), hereafter referred to as TRMMv7; and for the rest meteorological variables data were obtained from the Princeton Hydrology archive and consist of reanalysis data that have been post-processed and merged with observations (National Center of Environmental Predictions, Kalnay et al., 1996; Sheffield et al., 2006). The mean climatic CFs were based on monthly-mean climatological conditions over 6-year time slices from each of the 21 CMIP5 models: 2000-2005 for the historical CMIP5 model outputs, and 2006-2035 for RCP4.5 and RCP8.5. The CFs were used to rescale the historical observations at the daily time-scale. For a flow chart describing the method see Figure 5. The CFs were further interpolated to the 0.1 degree resolution of the 260 modelling setup, using the bilinear interpolation method.



The next step was to force JULES with the rescaled historical observations and generate future hydrological projections for the UG basin that go up to year 2035. Two different sets of modelling experiments were run: In the first one, only climate change was taken into account, as JULES was driven by the CMIP5 outputs of 21 models, under two emission scenarios (RCP4.5 & RCP8.5), but 265 land use was kept constant to historic year 2010 (see Section 2.4). In the second set, both climate change and land-use change were taken into consideration, as apart from the CMIP5 model outputs, JULES was also forced by a set of 15 year-to-year varying time-series of future land-use scenarios. The impact of both climate change and land-use change on the future hydrological variables of the study area is examined. Table 2 outlines all of the JULES runs as described above.



Table 2. Summary of the JULES experiments

LU maps CMIP5 outputs	Historic (2010)	Future projections (2010-2035) x 15
Historical (2000-2005)	X	
RCP4.5 (2006-2035)	X	X
RCP8.5 (2006-2035)	X	X

270 In the following sections, the subscript *_cl* corresponds to results produced by taking only climate
change into account, over the simulation period 2030-2035; the subscript *_cl_lu* corresponds to
results produced by taking into account both climate change and land-use change, over the simulation
period 2030-2035; and the subscript *_hist* corresponds to results from the historical simulation period
2000-2005.

275 4 Results

4.1 CMIP5 Projection analysis

280 A direct analysis of the monthly precipitation climatologies for the UG basin reveals large variations
between the different GCM precipitation datasets (Fig. 6). Interestingly, there are models that are
not able to capture at all the seasonal cycle and the summer monsoon precipitation, but instead re-
produce a flat annual climatology (likely due to poor representations of the annual cycle of monsoon
circulation). This illustrates the large uncertainties and questions the ability of some of the models
to represent the present-day climate. However, this is no straightforward indicator of their ability to
generate reasonable future climate projections.

285 The spatial patterns of precipitation change between the periods 1975-2005 and are
shown in Fig. 7. For the summer monsoon period (JJA), the multi-model mean (MMM) pattern of
future projections is pointing towards a precipitation increase of up to 2.4 mm/d under scenario
RCP4.5. As expected, under scenario RCP8.5, which corresponds to stronger radiative forcing, the
precipitation increase is stronger (up to 4.1 mm/d). For the dry period (DJF), under RCP4.5, the
MMM is projecting for some areas a small decrease in precipitation (up to -0.2 mm/d), whilst for
290 other areas projecting an increase of up to 0.36 mm/d. Similar but slightly stronger patterns of change
are observed for DJF under RCP8.5. This means that an amplification of the annual cycle is being
projected for the end of the century, with more pronounced wet and dry seasons.

295 Figure 8 shows the spatial patterns of temperature change between the periods 1975-2005 and
. The projections indicate a robust signal of temperature increase in all examined periods
and under both emission scenarios. The temperature increase ranges from 1.6 to 3.6°C under RCP4.5
and from 2.7 to 6.8°C under RCP8.5.

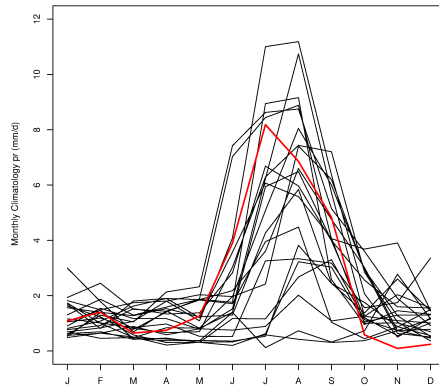


Figure 6. Monthly historical precipitation climatologies of the 21 CMIP5 models used in this study (black) and how they compare to the TRMMv7 satellite product (red), over the period 2000–2005 (the CMIP5 historical experiment ends in 2005). The data correspond to aerial averages, covering the extent of the UG basin.

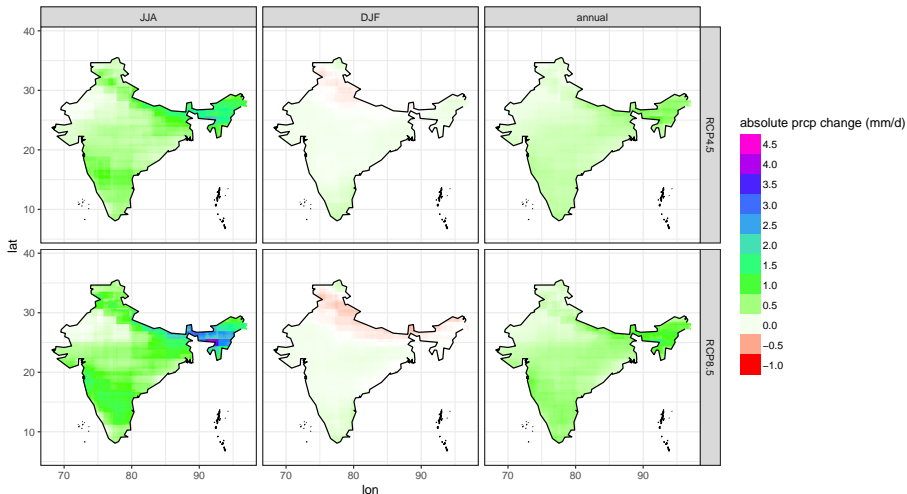


Figure 7. Absolute change [mm/d] in the multi-model mean precipitation over India between 1975–2005 and 2070–2100. Results are separated under 2 emission scenarios (RCP4.5 & RCP8.5) averaged over three different periods: the monsoon period (June–August, JJA), the dry winter period (December–February, DJF) and the annual period. The data were interpolated to the 0.1 degree resolution of the modelling setup, using the bilinear interpolation method.

Further details on the skill of the CMIP5 GCM models used in this study are available in Appendix A.

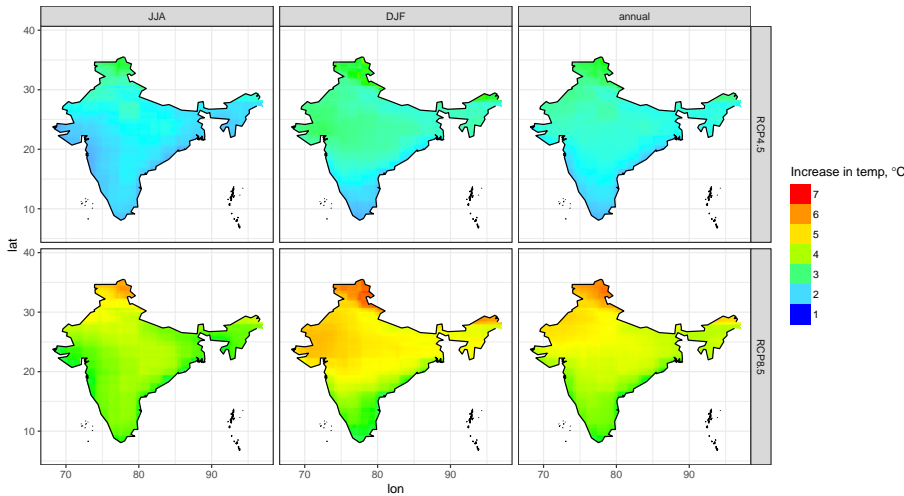


Figure 8. Absolute change [$^{\circ}\text{C}$] in the multi-model mean surface air temperature over India between 1975–2005 and 2070–2100. Results are separated under 2 emission scenarios (RCP4.5 & RCP8.5) and three different time-scales: the monsoon period (June–August, JJA), the dry winter period (December–February, DJF) and the annual period. The data were interpolated to the 0.1 degree resolution of the modelling setup, using the bilinear interpolation method.

4.2 Hydrological Projections

300 After forcing JULES with the down-scaled future climate projections from the CMIP5 multi-model database and in conjunction with estimates of different future land-use scenarios, we calculate variations in the following hydrological components: flows , evapotranspiration and soil moisture.

305 Focusing upon the MMM values (Fig. 9), for the entire UG basin, when only climate change is taken into consideration, the high flows exceeded only 5% of time (Q_5) are projected to increase in magnitude by 41% [SD=73, the standard deviation of the percent change] compared to historic values, under RCP4.5 and by 60% [SD=76] under RCP8.5 (Table 3).

310 When both climate change and land-use change are taken into account, the increase in the high extremes of flows is slightly higher: 42% [SD=72] increase under RCP4.5 and 63% [SD=72] increase under RCP8.5. In the low flows, the impact of climate change only is not as significant. Low flows exceeded 95% of time (Q_{95}) are decreased in magnitude by 2% [SD=28] under RCP4.5 and by 3% [SD=19] under RCP8.5. When land-use change is also taken into account, Q_{95} is projected to increase by 1% [SD=31] under RCP4.5 and to decrease by 1% [SD=17] under RCP8.5. So there is a clear impact of both climate change and land-use change in the high and low extremes of flows.



315 The small increase in future streamflows that is attributed to land-use change could be directly related to urbanisation (i.e. reduced infiltration and increased discharge), which is one of the main land-use change trends being projected for the future. On the other hand, it is possible that the impacts of urbanisation are cancelled out by the impacts of forest growth along with bare soil loss, which are less surface runoff and more ET.

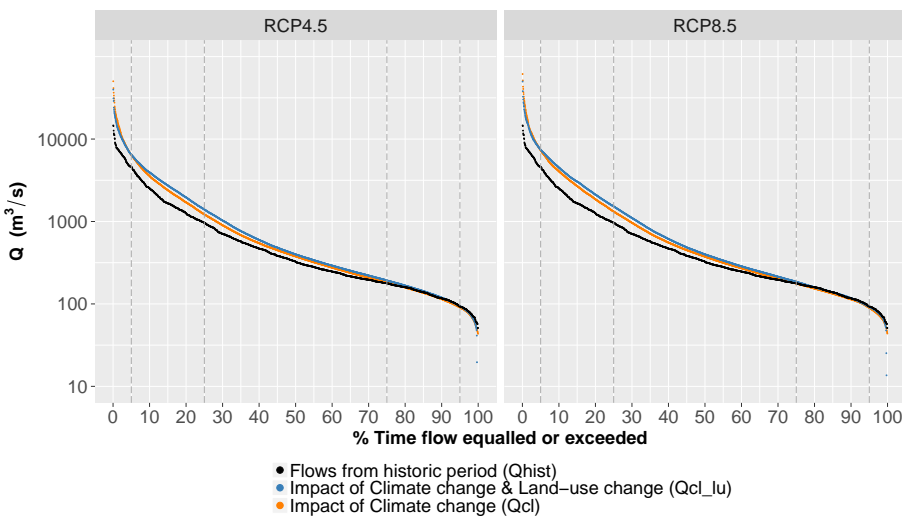


Figure 9. Flow duration curves of the streamflows simulated by JULES for the UG basin, at Kanpur barrage. Orange: Multi-model mean values when only climate change is taken into account (Q_{cl}), simulation period 2030-2035. Blue: Multi-model mean values when both climate change and land-use change are taken into account (Q_{cl_lu}), simulation period 2030-2035. Black: Historical period (Q_{hist}), simulation period 2000-2005.

Table 3. Q_5 and Q_{95} flow values (m^3/s) based on the flow duration curves shown in Figure 9

	Historical		RCP4.5		RCP8.5	
	Q_{hist}	Q_{cl}	Q_{cl_lu}	Q_{cl}	Q_{cl_lu}	
Q_5	4576	$6450 = 1.41 \times Q_{5hist}$ SD = 3346	$6504 = 1.42 \times Q_{5hist}$ SD = 3276	$7325 = 1.60 \times Q_{5hist}$ SD = 3477	$7443 = 1.63 \times Q_{5hist}$ SD = 3274	
Q_{95}	93	$91 = 0.98 \times Q_{95hist}$ SD = 26	$94 = 1.01 \times Q_{95hist}$ SD = 29	$90 = 0.97 \times Q_{95hist}$ SD = 17	$92 = 0.99 \times Q_{95hist}$ SD = 16	

320 Spatial changes of ET between the historical (2000-2005) and future projection period (2030-2035), under both emission scenarios (RCP4.5 & RCP8.5) are shown in Fig. 10. Results are split into 3-month period seasonalities for winter (DJF), spring (MAM) and summer (JJA), under the two types of experiments: (a) only climate change is taken into account (ET_{cl}), and (b) both climate change and land-use change are taken into account (ET_{cl_lu}). The differences between ET_{cl} and ET_{cl_lu} are very small in all seasons examined. The highest increase in ET (0.8mm/d) is projected

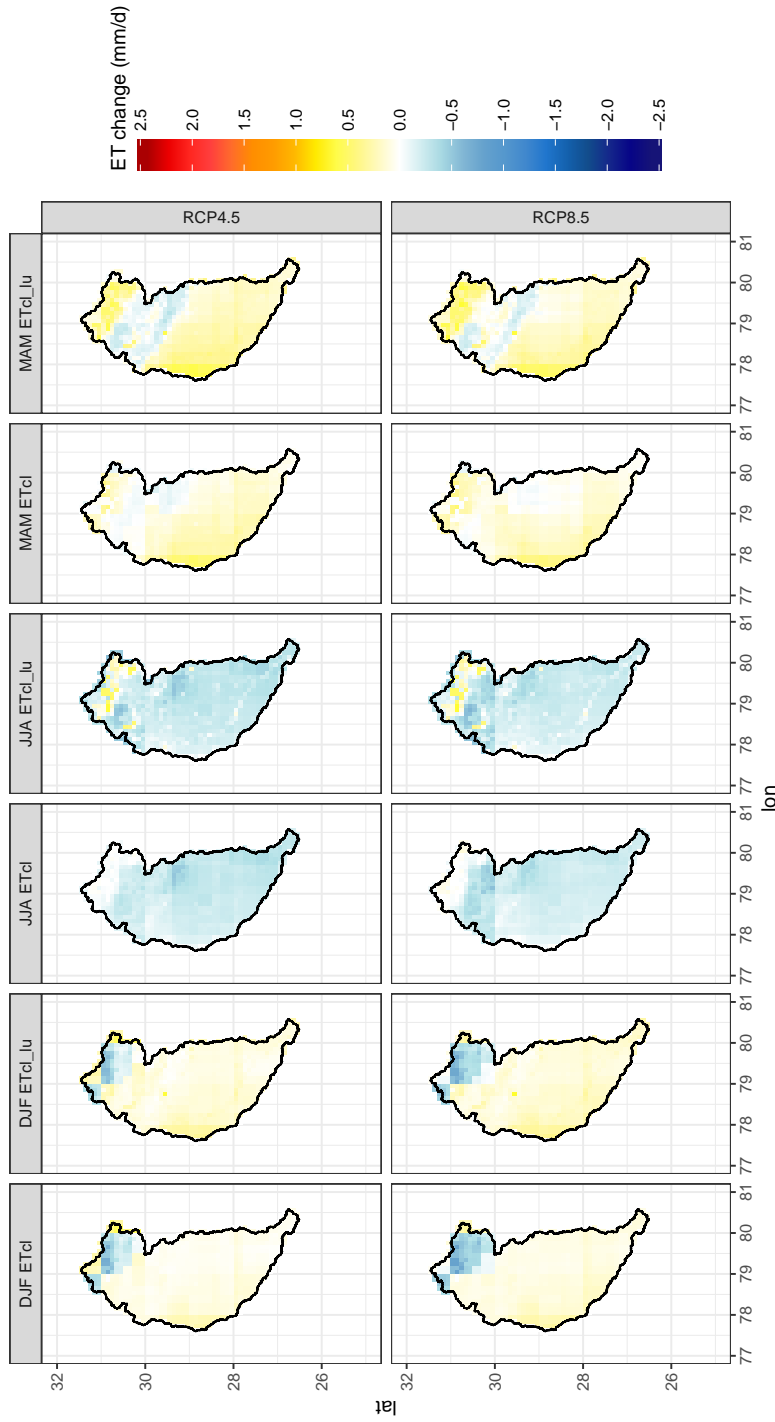


Figure 10. Absolute changes of spatial evapotranspiration (ET) fluxes between the historical simulation period 2000–2005 and the future projection simulation period 2030–2035, for the UG basin and for each of the emission scenarios (RCP4.5 & RCP8.5). Results are split into 3-month period seasonalities for winter (DJF), spring (MAM) and summer (JJA), under the two types of experiments: (a) only climate change is taken into account (ETcl), and (b) both climate change and land-use change are taken into account (ETcl_{lu}).



to occur during spring in the southern agricultural parts of the catchment. The highest decrease in ET (-0.9mm/d) is projected to occur during the spring and summer periods in the mid-north parts of the study area. Nonetheless, those changes (Fig. 12 & 19) are cancelled out when spatially averaged across the catchment results are presented (Fig. 13 & 20).

330 In terms of spatial changes of soil moisture, it is shown in Fig. 11 that similarly to the patterns of ET change, the highest increase in MMM soil moisture (4 kg m^{-2}) is projected to occur during spring, in the southern agricultural parts of the catchment. The highest decrease in soil moisture (-10 kg m^{-2}) is projected to occur during the winter and summer periods, in the mid-north parts of the study area. However, it seems that these changes of soil moisture are cancelled out when spatially averaged results are presented (Fig. 13 & 20).

Note that for the projections of ET and soil moisture fluxes, the differences between the two RCP scenarios are not large. In the nearby-future period examined here (2030-2035), the relative importance of the RCPs is far smaller than the GCM model uncertainties.

340 Further details on the hydrological projections developed for this study are available in Appendix B.

5 Discussion

345  Overall, climate change is the main driver of hydrological change in the near term future scenarios explored in this study. If no dramatic land-use changes take place in the nearby future, the main alterations in hydrological fluxes are expected to arise from the change in the meteorology (and mainly precipitation). The relative contribution of land-use change is of an approximate magnitude of 2% change compared to historic values. However, the strong inter-model uncertainties of the future projections (see SD values in Section 4.2 and Table 3), which were possibly amplified by the delta-change approach, are posing a limitation to the confidence of these results. Nevertheless, as GCM uncertainties are unlikely to decrease quickly, decisions on the adaptation and mitigation of 350 climate change should not be delayed (Knutti and Sedlacek, 2013).

Future projections in relation to water demand

This section places the above results in a water resources context, by discussing the implications of climate change on the water resources of the Upper Ganges and whether it is likely that water demand thresholds (i.e. amount of water that sustains environmental flows and water consumption) 355 of the region will be exceeded in the future. A recent study by Sapkota et al. (2013) presented mean monthly water demands for irrigation, industrial and domestic purposes (period 1991-2005), in the UG basin. According to this study, irrigation water demands from canals (which are much higher compared to industrial and domestic demands) are low during the monsoon period from June to September and high from November to February. During the winter months December and January,

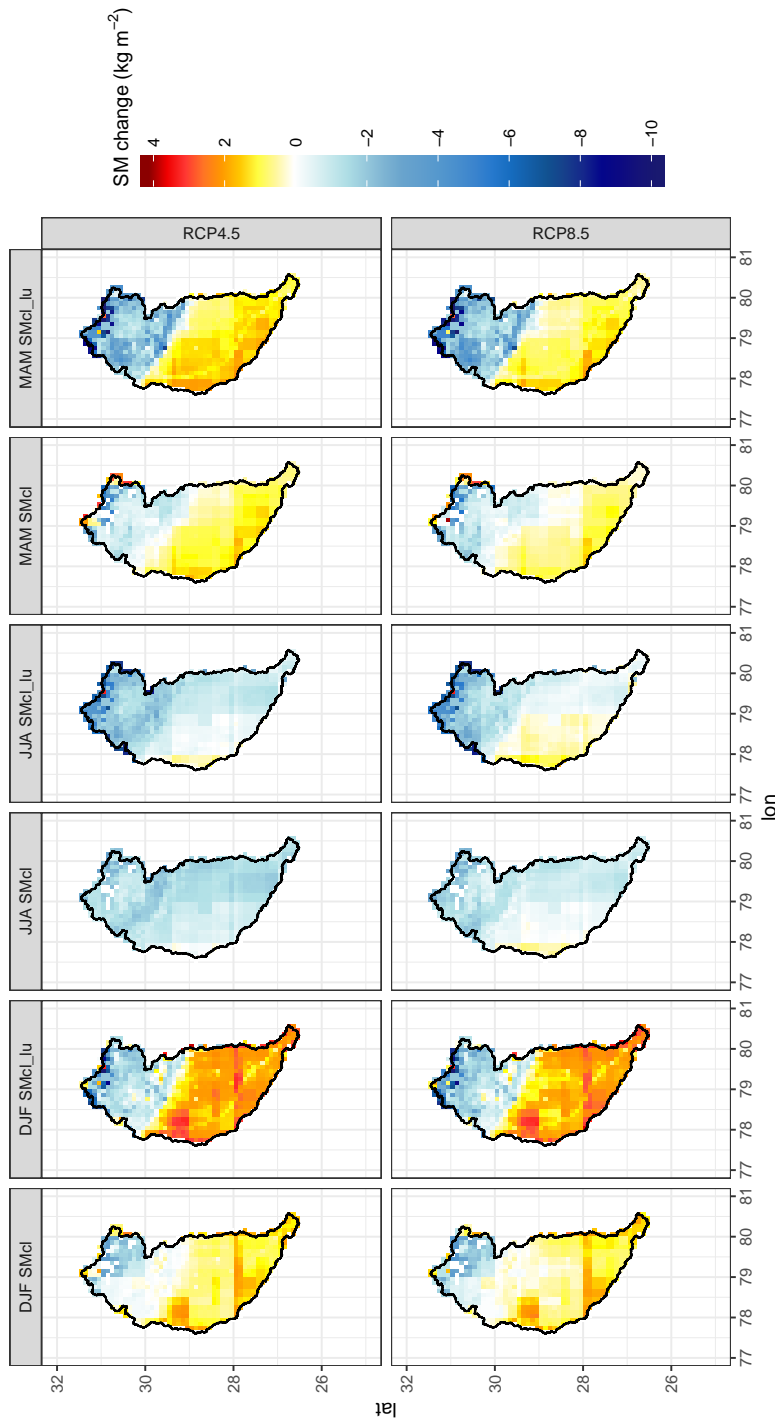


Figure 11. Absolute changes of spatial soil moisture (SM) fluxes between the historical simulation period 2000-2005 and the future projection simulation period 2030-2035, for the UG basin and for each of the emission scenarios (RCP4.5 & RCP8.5). Results are split into 3-month period seasonalities for winter (DJF), spring (MAM) and summer (JJA), under the two types of experiments: (a) only climate change is taken into account (SMcl), and (b) both climate change and land-use change are taken into account (SMcl_lu).

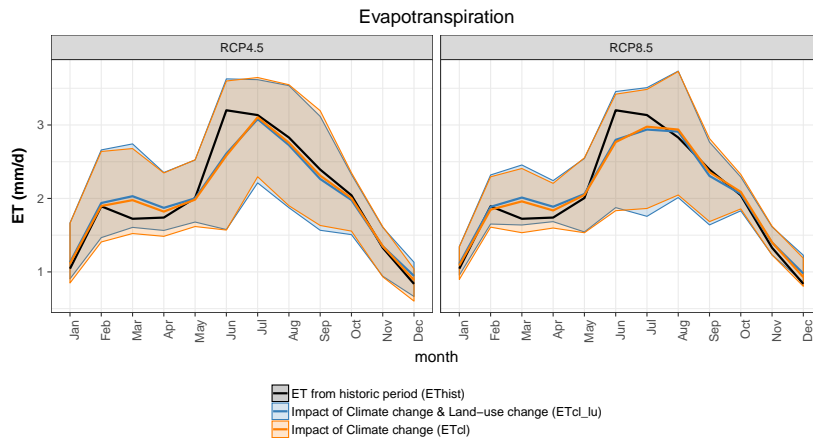


Figure 12. Multi model mean values of the ET fluxes simulated by JULES, for the UG basin and for each of the emission scenarios (RCP4.5 & RCP8.5). Black colour corresponds to the historical simulation period 2000-2005 (ET_{hist}). Orange colour corresponds to the simulation period 2030-2035, when only climate change is taken into account (ET_{cl}). Blue colour corresponds to the simulation period 2030-2035, when both climate change and land-use change are taken into account (ET_{cl_lu}). Shaded areas correspond to the max and min ET values obtained from different GCM forcings and illustrate the large CMIP5 model spread.

360 water demand in the UG basin is already unmet. In recent years pressure has increased on the river canals to maintain flows during the dry season, due to the introduction of high water intensive crops, agricultural expansion and population growth (Sapkota et al., 2013).

361  Here, the mean monthly water demands shown in Fig.4 of Sapkota et al. (2013) are used in combination with future projections of changes in India's water demands, as presented in the study by 362 Amarasinghe et al. (2007). This study suggests an expected 8% increase in surface water demand for irrigation, 130% increase in surface water demand for domestic usage and 152% increase in surface water demand for industrial usage, by 2030 under a business as usual scenario, which is mainly extrapolating trends of recent years (calculations after linearly interpolating results presented for years 2025 and 2050).

370 Based on the two studies mentioned above, future projections of surface water demand for the UG basin were generated, on a monthly basis and for the period 2030-2035. Figure 14 shows how the future expected surface water demand compares with the flow volumes as calculated by JULES (period 2030-2035) under the two examined RCP scenarios, when only climate change is taken into account and when both climate change and land-use change are taken into account. Since the 375 main months under water stress are those in the dry season, and in order to better visualise the results outside the wet summer period (which is dominated by high flows), the y axis was limited to values lower than 2000 million m³ of water. The future winter months (Dec-Feb) are expected to be

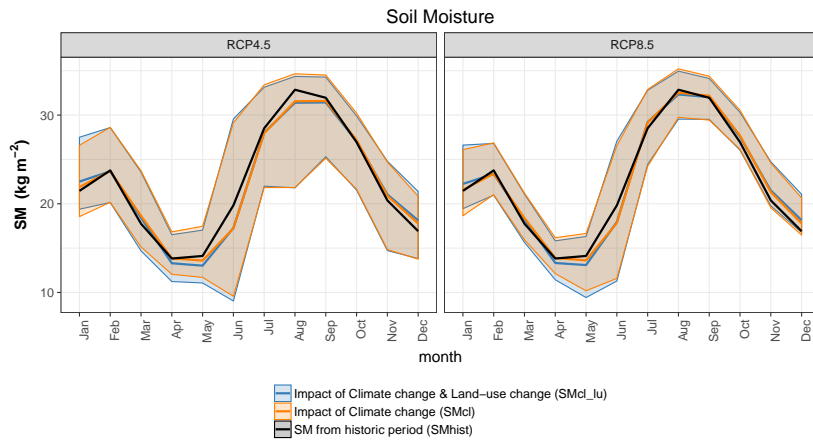


Figure 13. Multi model mean values of the SM fluxes simulated by JULES, for the UG basin and for each of the emission scenarios (RCP4.5 & RCP8.5). Black colour corresponds to the historical simulation period 2000-2005 (SM_{hist}). Orange colour corresponds to the simulation period 2030-2035, when only climate change is taken into account (SM_{cl}). Blue colour corresponds to the simulation period 2030-2035, when both climate change and land-use change are taken into account (SM_{cl_lu}). Shaded areas correspond to the max and min SM values obtained from different GCM forcings and illustrate the large CMIP5 model spread.

most problematic in terms of meeting the surface water demands, with agriculture being the main water user. This poses threats to the river's capacity to maintain flows at an acceptable ecological level (environmental flows) during those months. Sapkota et al. (2013) showed that using less water intense crops in the UG basin, is more efficient than reducing the total agricultural area by 40%, in reducing the unmet irrigation water demands. Besides, as previously discussed but also shown in Fig. 14, the main driver of future change in water resources is not land-use change. It is climate change but also the changing practices within certain types of land-use (i.e. increased irrigation efficiency, upstream dams) that are expected to drive changes in the future water availability of the UG basin, rather than land-use change per-se.

Understanding the future water availability in India is much more complex than looking from the perspective of climate and land-use change only. For instance, India is one of the greatest hydropower generators in Asia. A potential future increase in hydropower capacity, aside from its large benefits in terms of reducing carbon emissions, brings further environmental concerns regarding river flows, water quality and eco-diversity. Therefore, the impacts of such water management decisions (e.g. hydropower dam structures) could also play a major role in the water balance of this region.

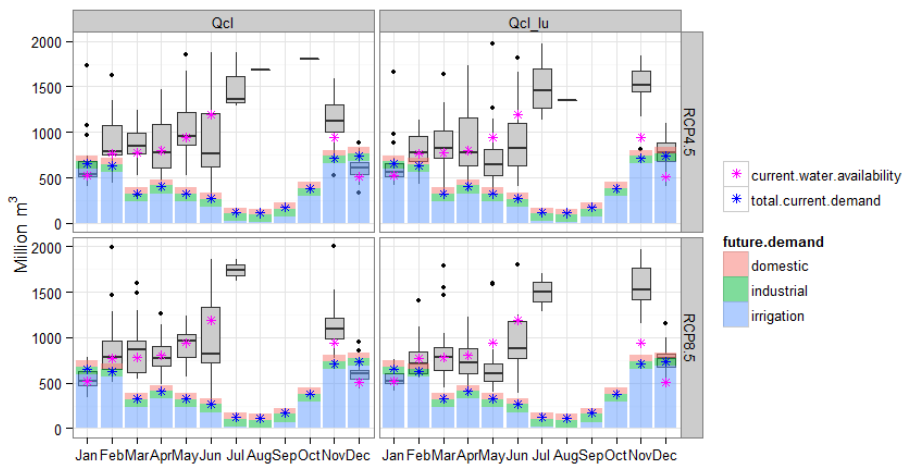


Figure 14. Bars showing future projections of monthly surface water demand, for irrigation, domestic and industrial usage, during the period 2030-2035, for the UG basin. Box plots indicate monthly flow volumes calculated by JULES under different GCM forcings, for the same period. The demand data are based on figures presented in the studies by Sapkota et al. (2013) and Amarasinghe et al. (2007), as discussed above.

6 Conclusions

In this study, the impact of land-use change and climate change on the future hydrology of the
 395 UG basin was assessed by calculating annual variations in hydrological components (stream flow, evapotranspiration and soil moisture). Two sets of modeling experiments were run in the JULES land-surface model, covering the period 2000-2035: (a) the model was forced with future climate projections from the CMIP5 multi-model database, whilst land use was kept constant to historic year 2010; (b) the model was forced with future climate projections from the CMIP5 multi-model
 400 database, in conjunction with estimates of 15 future land-use scenarios, based on Landsat satellite images and Markov chain analysis.

Large variations between GCM-derived precipitation datasets arise from a basic analysis of CMIP5 model outputs. A stronger wet season is projected to occur by the end of the century according to MMM values.

405 Significant differences between the historic and nearby-future hydrologic fluxes arise under future land-cover and climate change scenarios, pointing towards a severe increase in high extremes of flow.
Using the period 2030–2035, Q_5 is projected to increase by up to 42% [SD=72] under RCP4.5 and by up to 63% [SD=72] under RCP8.5, compared to historic values of the period 2000–2005. The changes in all examined hydrological components are slightly greater in the combined land-use and
 410 climate change scenario compared to the stand-alone climate change scenario. However, the main



driver of future hydrological change is climate change. In terms of spatial changes in ET and SM, the changes that occur in various parts of the catchment are cancelled out by changes of the opposite direction, occurring in different parts of the catchment, leading to smaller overall changes in terms of aerial averages.

415 The large uncertainties in the CMIP5 model outputs were possibly amplified by the delta-change approach followed here and led to a large spread of results for the future hydrological variables (e.g. Figs 12 & 13, SD values in Section 4.2 and Table 3). Nonetheless, as GCM uncertainties are unlikely to decrease in the near future, this work could help prioritize adaptation strategies and regional land-use planning to improve northern India's water resources.

420 Lastly, the results were presented in a water resources context, with the aim of understanding what climate and land-use change mean for the future water resources of the UG basin. When looking into future water availability and demand (period 2030–2035), the river's capacity to maintain ecological flows during the dry season is threatened. It is however important to highlight that under a changing climate, it is not land-use change per se that is expected to drive changes in the water re-
425 sources availability but changing practices within certain types of land use (i.e. improved crop water productivity), that could significantly impact future water needs.

Appendix A: CMIP5 Projection analysis

A Taylor diagram is used to assess the relative skill of the CMIP5 models used in this study and estimate which of them performs better, in terms of simulating historical precipitation patterns over the
430 study area (Fig. 15). The diagram quantifies the similarity between modelled and observed precipitation in terms of spatial pattern correlation coefficient, standard deviation and centred root-mean-square (RMS) difference (Taylor, 2001). Figure 15 graphically summarises how closely the historic precipitation generated by each of the 21 CMIP5 models used in this study matches TRMMv7 observed precipitation, over the period 2000–2005. This plot illustrates that for the specific time period
435 of 2000–2005, models such as CNRM-CM5, MIROC4h, MIROC5 are perceived to outperform models like IPSL-CM5B-LR or CSIRO-Mk-3-6-0 in terms of their ability to match TRMMv7 observed precipitation well.

Figure 16 shows the CFs of precipitation relative to the historic period 2000–2005, averaged in the UG basin. It is evident that the spread of the results is large, and many models show opposite
440 directions of change. Nevertheless, all the mean values point towards an increased precipitation for all months. The uncertainty is higher for the dry months November and December, which have the highest % increase in precipitation relative to historic values. On the other hand, the spread seems to be narrower for the wet summer months but nonetheless there are still models with contrasting results.

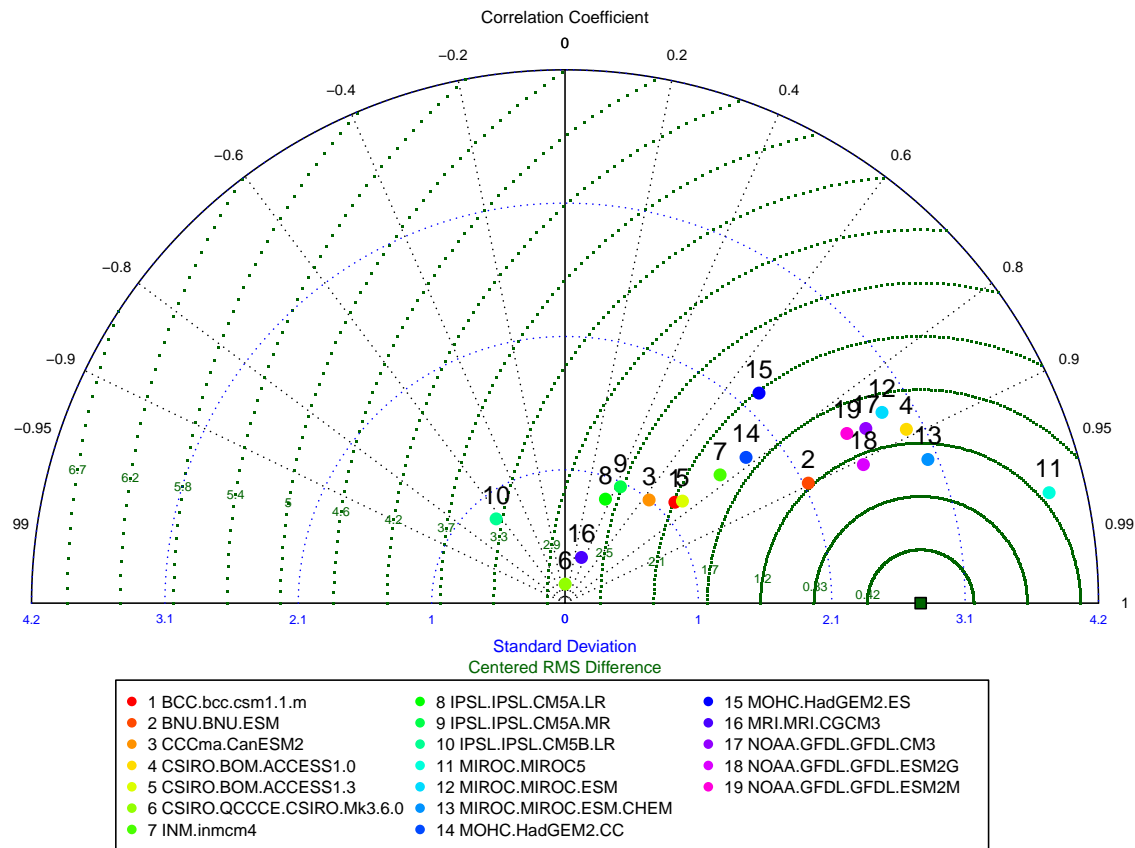


Figure 15. Taylor diagram that graphically summarises how closely the historic precipitation generated by each of the 21 CMIP5 models used in this study matches TRMMv7 observed precipitation, over the period 2000–2005. According to that diagram, the closer a model is to the observation (dark green - squared dot in the bottom right side of graph), the better it performs.

445 Appendix B: Hydrological Projections

The generated streamflows (Fig. 17) reveal the impact of both climate change and land-use change in the future flows. The spread of the results is indicative of the uncertainties among different GCM forcing data. The spread is large under both emission scenarios, which suggests that the GCM precipitation spread is relatively less sensitive to the level of radiative forcing. Further, it is noticeable 450 that the agreement in projections of low flows is stronger than that of high flows, because the future projections of extreme precipitation events have large uncertainties in the tropical regions as also mentioned in the study by Kharin et al. (2013).

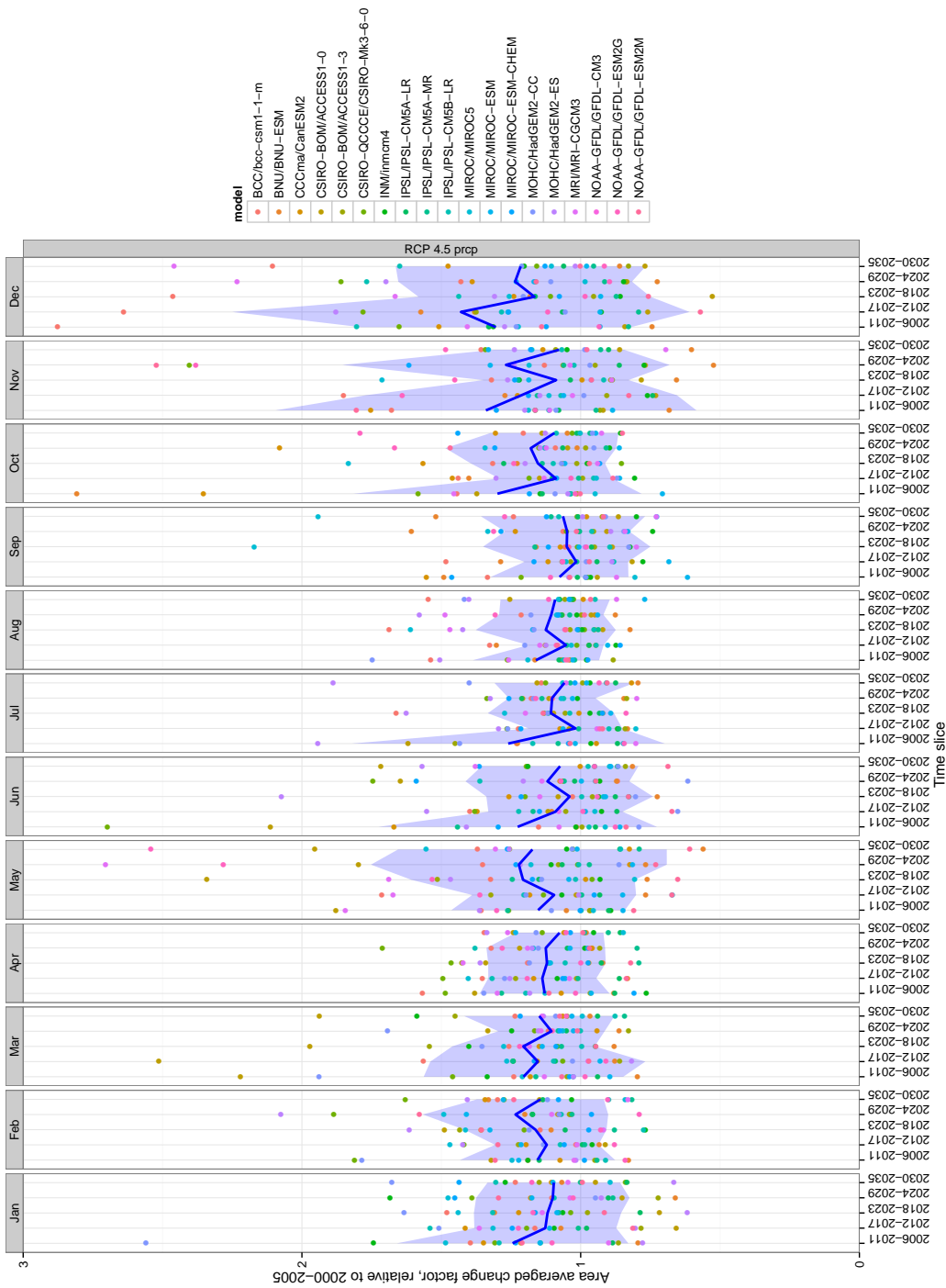


Figure 16. 6-year CDFs of precipitation in the UG basin. Each dot represents the basin's areal average of a particular model. The precipitation anomalies are relative, unit-less values. A higher than 1 value indicates an increase and a smaller than 1 value indicates a decrease of precipitation. The blue line represents the mean value whereas the shading represents the spread of projections from the multi-model ensemble.

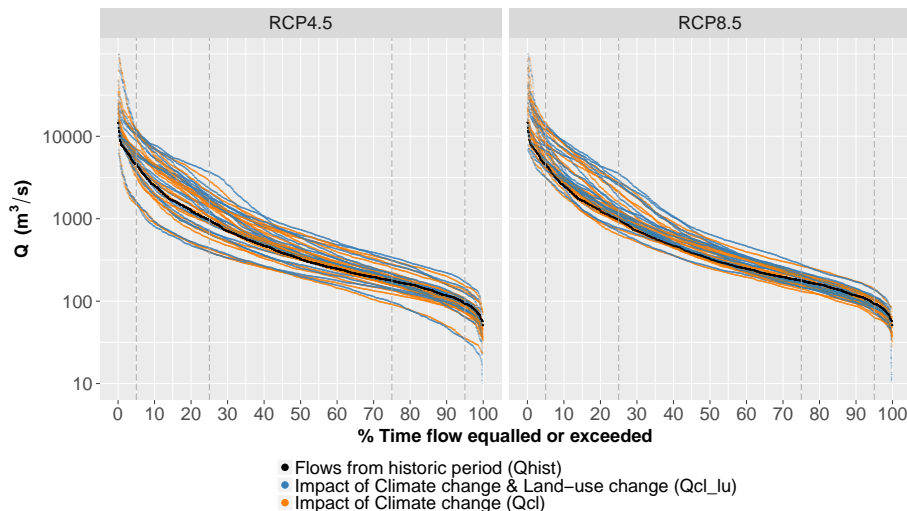


Figure 17. Flow duration curves of the streamflows simulated by JULES for the UG basin, when forced by CMIP5 model outputs. Orange: only climate change is taken into account (Q_{cl}), simulation period 2030-2035, each line represents JULES outputs based on different CMIP5 model forcing. Blue: both climate change and land-use change are taken into account (Q_{cl_lu}), simulation period 2030-2035, each line represents JULES outputs based on different CMIP5 model forcing. Black: Historical period (Q_{hist}), simulation period 2000-2005.

Kernel density plots shown in Fig. 18 show the distributions of Q_5 , Q_{25} , Q_{50} , Q_{75} , Q_{95} , (i.e. flows exceeded 5%, 25%, 50%, 75% and 95% of time respectively), among different GCMs, when only 455 climate change is taken into account (Q_{cl}) and when both land-use and climate change are taken into account (Q_{cl_lu}), for the UG basin. The large variations of flows highlight the large spread among GCM outputs used to force JULES. It is evident that the differences between the two RCPs are greater than the differences between Q_{cl} and Q_{cl_lu} of the same RCP. As illustrated by the densities 460 shown in Fig. 18, the agreement in projections of low flows (Q_{75} , Q_{95}) is stronger than that of high flows (Q_5 , Q_{25}), as previously discussed.

The magnitude of increase in the future projections of streamflows might appear unrealistic, and 465 this is partly attributed to the downscaling method used that increased precipitation extremes and partly to the uncertainties of GCM outputs. The mean climatic CFs were calculated from the mean monthly climatologies over 6-year time slices. However, given the large variability of precipitation on daily time-scales compared to the mean monthly climatology, by scaling the high extremes of precipitation according to the CF, it is inevitable that in some cases precipitation is highly exaggerated in the future projections. In such a large catchment inflated precipitation extremes would be directly translated by JULES into unreasonably high runoff values. Nevertheless, there is qualitative

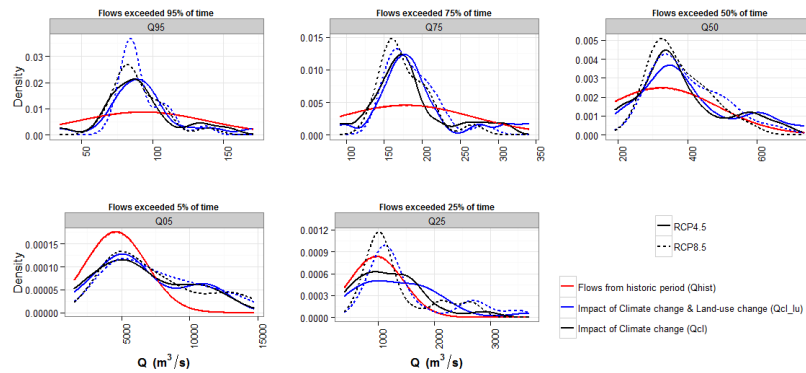


Figure 18. Kernel density plots showing distribution of Q_5 , Q_{25} , Q_{50} , Q_{75} , Q_{95} (i.e. flows exceeded 5%, 25%, 50%, 75% and 95% of time respectively), among different GCMs, for the UG basin, under both emission scenarios. Black: Only climate change is taken into account (Q_{cl}), simulation period 2030-2035. Blue: Both climate change and land-use change are taken into account (Q_{cl_lu}), simulation period 2030-2035. Red: Historical period (Q_{hist}), simulation period 2000-2005.

similarity between results shown here and results presented by Lutz et al. (2014), who found that for
 470 the UG basin, projected precipitation increases during the monsoon period, could lead to increases
 in total annual runoff up to 10% for RCP4.5 and 27% for RCP8.5, during the period 2041–2050.

In terms of ET fluxes (Fig 12), the MMM future projections under RCP4.5 are pointing towards
 increased ET for the spring months March and April and decreased ET over the summer period
 (June–September). Under RCP8.5, ET follows similar patterns of change, although in August the
 475 projection is pointing towards increased ET compared to historic values. In all cases, it is evident
 that in the near-term future projections, the inter-model uncertainty is higher than the scenario un-
 certainty. This is also shown in Fig 19, which displays monthly percentage changes of ET between
 historic (2000–2005) and future period (2030–2035), spatially averaged in the UG basin. The spread
 of results derived by JULES forced with different GCM outputs is large under both RCPs but the
 480 MMM changes are never higher than 20%.

On the other hand, the MMM future projections of soil moisture under the same scenario (Fig 13)
 show a decrease in soil moisture from April to September. Interestingly, the changes of soil moisture
 relative to the historic period are smaller under RCP8.5 compared to RCP4.5. The overall agreement
 between historic and both future scenarios seems to be better in the soil moisture results compared to
 485 the ET results (see also the spread of results in Figs. 19–20). Figure 20, displays monthly percentage
 changes of soil moisture between historic (2000–2005) and future projections period (2030–2035),
 spatially averaged in the UG basin. It is shown that the spread of results is larger under RCP4.5
 compared to RCP8.5. This could be explained by the stronger forcing of the RCP8.5, which leads



the GCMs to produce more similar results. In all cases the MMM changes between historic and
490 future projections in soil moisture are never higher than approximately 20%.

As previously mentioned, it seems that the projected for the future increase in precipitation is
translated as more intense precipitation events (due to the delta-change approach followed here).
Besides, the differences between the two RCP scenarios are not large, especially for the projections
of ET and soil moisture fluxes. In the nearby-future period examined here (2030-2035), the relative
495 importance of the RCPs is far smaller than the GCM model uncertainties. Finally, it is important to
note that this study did not explicitly address future changes in irrigation practices that could have a
large impact in ET rates over the study area.

Acknowledgements. G. Tsarouchi acknowledges support by the Grantham Institute for Climate Change (Imperial College London) and HR Wallingford. W. Buytaert acknowledges support by the NERC Changing Water
500 Cycle (South Asia) project Hydrometeorological feedbacks and changes in water storage and fluxes in Northern India (grant number NE/I022558/1). We also acknowledge the World Climate Research Programme's Working Group on Coupled Modelling, which is responsible for CMIP, and we thank the climate modeling groups (listed in Table 1 of this paper) for producing and making available their model output. For CMIP the U.S. Department of Energy's Program for Climate Model Diagnosis and Intercomparison provides coordinating support and led
505 development of software infrastructure in partnership with the Global Organization for Earth System Science Portals.”

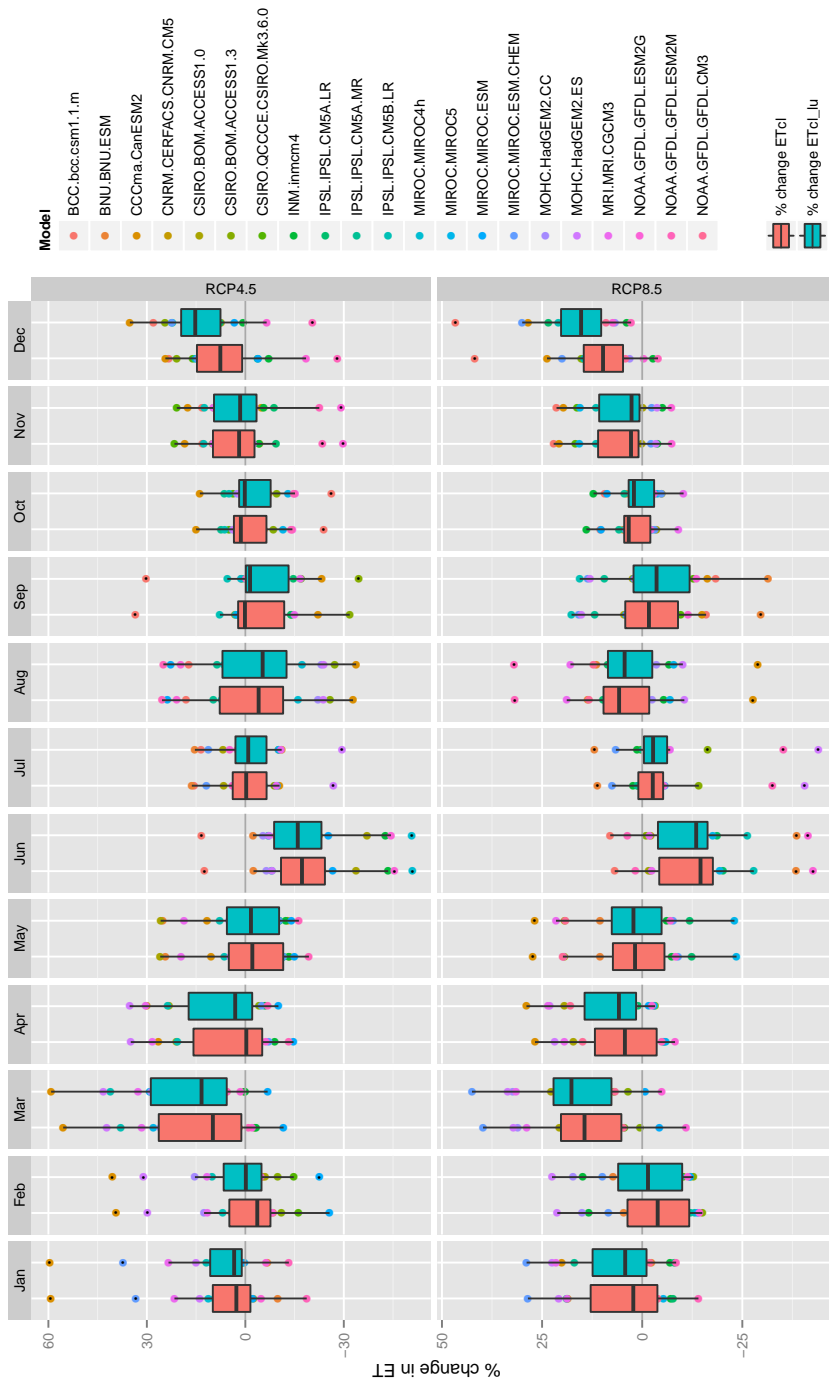


Figure 19. Percentage changes of evapotranspiration (ET) fluxes between the historical simulation period 2000–2005 and the future projection simulation period 2030–2035, for the UG basin and for each of the emission scenarios (RCP4.5 & RCP8.5). Pink colour corresponds to the scenarios that only climate change is taken into account. Blue colour corresponds to the scenarios that both climate change and land-use change are taken into account.

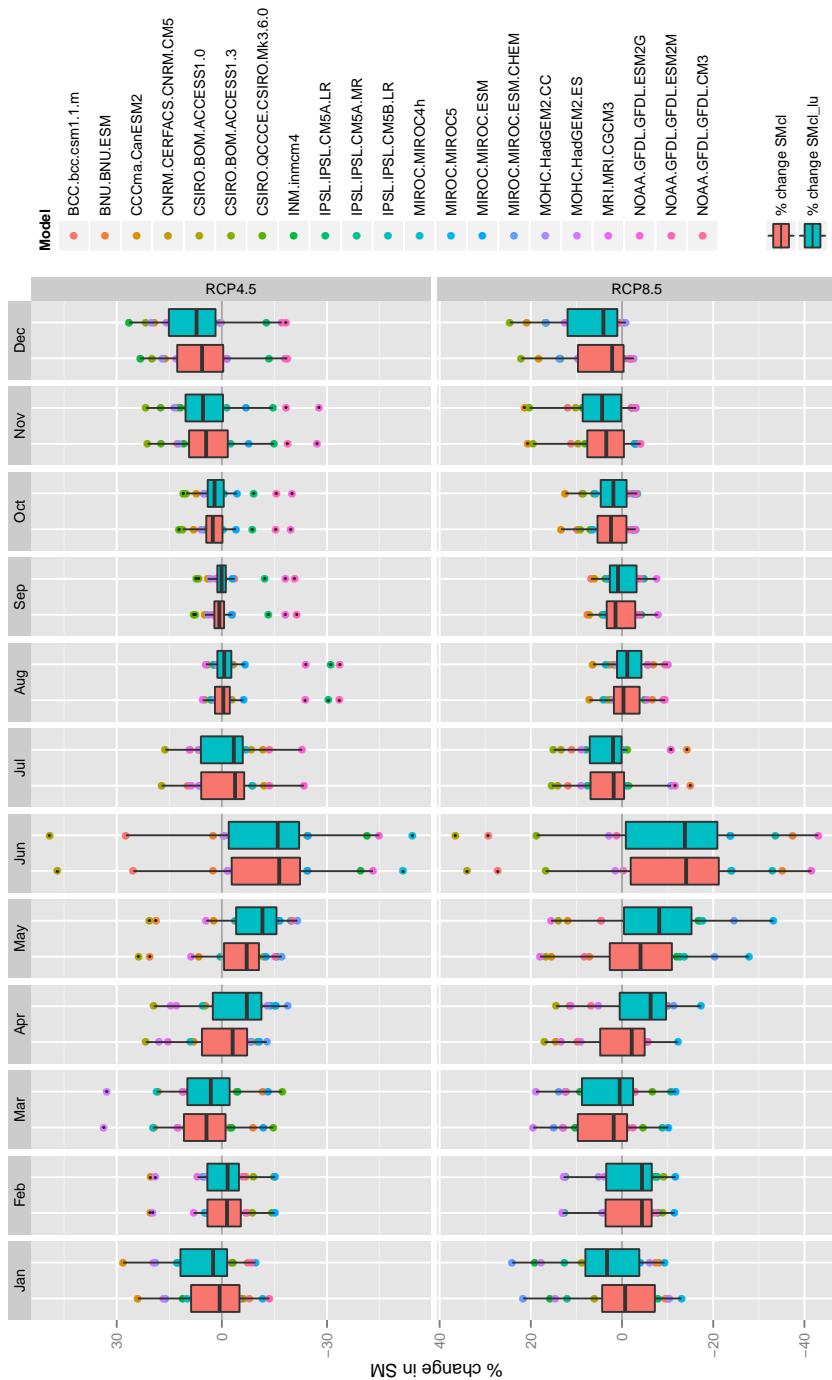


Figure 20. Percentage changes of soil moisture (SM) fluxes between the historical simulation period 2000–2005 and the future projection simulation period 2030–2035, for the UG basin and for each of the emission scenarios (RCP4.5 & RCP8.5). Pink colour corresponds to the scenarios that only climate change is taken into account. Blue colour corresponds to the scenarios that both climate change and land-use change are taken into account.



References

Amarasinghe, U., A., Shah, T., Anand, B. K., and Hugh, T.: India's water future to 2025-2050: business-as-usual scenario and deviations, International Water Management Institute, 2007.

510 Best, M. J., Pryor, M., Clark, D. B., Rooney, G. G., Essery, R. L. H., Menard, C. B., Edwards, J. M., Hendry, M. A., Porson, A., Gedney, N., Mercado, L. M., Sitch, S., Blyth, E., Boucher, O., Cox, P. M., Grimmond, C. S. B., and Harding, R. J.: The Joint UK Land Environment Simulator (JULES), Model description - Part 1: Energy and water fluxes, Geoscientific Model Development Discussions, 4, 595–640, <http://www.geosci-model-dev-discuss.net/4/595/2011/>, 2011.

515 Bharati, L., Lacombe, G., Gurung, P., Jayakody, P., Hoanh, C. T., and Smakhtin, V.: The impact of water infrastructure and climate change on the hydrology of the Upper Ganges River basin., International Water Management Institute; Colombo; Sri Lanka, http://www.iwmi.cgiar.org/Publications/IWMI_Research_Reports/PDF/PUB142/RR142.pdf, 2011.

Bhat, G. S.: The Indian drought of 2002 - a sub-seasonal phenomenon?, Quarterly Journal of the Royal Meteorological Society, 132, 2583–2602, doi:10.1256/qj.05.13, <http://dx.doi.org/10.1256/qj.05.13>, 2006.

520 Dash, S. K., Kulkarni, M. A., Mohanty, U. C., and Prasad, K.: Changes in the characteristics of rain events in India, Journal of Geophysical Research: Atmospheres, 114, doi:10.1029/2008JD010572, <http://dx.doi.org/10.1029/2008JD010572>, 2009.

Essery, R., Best, M., Betts, R., and Taylor, C.: Explicit representation of subgrid heterogeneity in a GCM land surface scheme, Journal of hydrometeorology, 4, 530–543, 2003.

525 Fowler, H. J., Blenkinsop, S., and Tebaldi, C.: Linking climate change modelling to impacts studies: recent advances in downscaling techniques for hydrological modelling, International Journal of Climatology, 27, 1547–1578, doi:10.1002/joc.1556, <http://dx.doi.org/10.1002/joc.1556>, 2007.

Huffman, G. J. and Bolvin, D. T.: TRMM and other data precipitation data set documentation., ftp://precip.gsfc.nasa.gov/pub/trmmdocs/3B42_3B43_doc.pdf, accessed: Nov 2013, 2013.

Huffman, G. J., Bolvin, D. T., Nelkin, E. J., Wolff, D. B., Adler, R. F., Gu, G., Hong, Y., Bowman, K. P., and Stocker, E. F.: The TRMM Multisatellite Precipitation Analysis (TMPA): Quasi-Global, Multiyear, Combined-Sensor Precipitation Estimates at Fine Scales, J. Hydrometeorol, 8, 38–55, 2007.

530 Immerzeel, W. W., van Beek, L. P. H., and Bierkens, M. F. P.: Climate change will affect the Asian water towers, Science, 328, 1382–1385, doi:10.1126/science.1183188, <http://www.sciencemag.org/content/328/5984/1382.abstract>, 2010.

IPCC: Climate Change 2013: The Physical Science Basis. Contribution of Working Group I to the Fifth Assessment Report of the Intergovernmental Panel on Climate Change , 2013.

IPCC: Climate Change 2014: Impacts, Adaptation, and Vulnerability. Part B: Regional Aspects. Contribution 540 of Working Group II to the Fifth Assessment Report of the Intergovernmental Panel on Climate Change , 2014.

Jain, S. K., Agarwal, P. K., and Singh, V. P.: Hydrology and Water Resources of India. Series: Water Science and Technology Library, Vol. 57, Springer, 2007.

Jenson, S. K. and Domingue, J. O.: Extracting Topographic Structure from Digital Elevation Data for Geographic Information System Analysis., Photogrammetric Engineering and Remote Sensing, 54, 1593–1600., 1988.



Kala, C. P.: Deluge, disaster and development in Uttarakhand Himalayan region of India: Challenges and lessons for disaster management, *International Journal of Disaster Risk Reduction*, 8, 143 – 152, doi:<http://dx.doi.org/10.1016/j.ijdrr.2014.03.002>, <http://www.sciencedirect.com/science/article/pii/S2212420914000235>, 2014.

550 Kalnay, Kanamitsu, Kistler, et al.: The NCEP/NCAR 40-Year Reanalysis Project, *Bulletin of the American Meteorological Society*, 77, 1996.

Kaushal, N. and Kansal, M.: Overview of water allocation practices in Uttar Pradesh and Uttarakhand with a specific reference to future demands., *SAWAS*, 2, 27–43, 2011.

555 Kharin, V., Zwiers, F., Zhang, X., and Wehner, M.: Changes in temperature and precipitation extremes in the CMIP5 ensemble, *Climatic Change*, 119, 345–357, doi:[10.1007/s10584-013-0705-8](https://doi.org/10.1007/s10584-013-0705-8), <http://dx.doi.org/10.1007/s10584-013-0705-8>, 2013.

Knutti, R. and Sedlacek, J.: Robustness and uncertainties in the new CMIP5 climate model projections, *Nature Clim. Change*, 3, 369–373, <http://dx.doi.org/10.1038/nclimate1716>, 2013.

560 Kumar, R., Singh, R. D., and Sharma, K. D.: Water resources of India., *Current Science*, 89, 794–811., 2005.

Lau, W. K. M. and Kim, K.-M.: The 2010 Pakistan Flood and Russian Heat Wave: Teleconnection of Hydrometeorological Extremes, *J. Hydrometeorol.*, 13, 392–403, doi:[10.1175/JHM-D-11-016.1](https://doi.org/10.1175/JHM-D-11-016.1), <http://dx.doi.org/10.1175/JHM-D-11-016.1>, 2011.

Lutz, A. F., Immerzeel, W. W., Shrestha, A. B., and Bierkens, M. F. P.: Consistent increase in High Asia's runoff due to increasing glacier melt and precipitation, *Nature Clim. Change*, 4, 587–592, <http://dx.doi.org/10.1038/nclimate2237>, 2014.

565 Maraun, D., Wetterhall, F., Ireson, A. M., Chandler, R. E., Kendon, E. J., Widmann, M., Brieren, S., Rust, H. W., Sauter, T., Themasl, M., Venema, V. K. C., Chun, K. P., Goodess, C. M., Jones, R. G., Onof, C., Vrac, M., and Thiele-Eich, I.: Precipitation downscaling under climate change: Recent developments to bridge the gap between dynamical models and the end user, *Reviews of Geophysics*, 48, doi:[10.1029/2009RG000314](https://doi.org/10.1029/2009RG000314), <http://dx.doi.org/10.1029/2009RG000314>, 2010.

Meehl, G. A., Arblaster, J. M., and Tebaldi, C.: Understanding future patterns of increased precipitation intensity in climate model simulations, *Geophys. Res. Lett.*, 32, L18 719, 2005.

Office of the Registrar General & Census Commissioner, India: *Census-2011*, <http://www.censusindia.gov.in>, 2011.

575 O'Keeffe, J., Kaushal, N., Smakhtin, V., and Bharati, L.: Assessment of environmental flows for the Upper Ganga basin, Technical report, WWF-India, Delhi, 2012.

Piani, C., Weedon, G., Best, M., Gomes, S., Viterbo, P., Hagemann, S., and Haerter, J.: Statistical bias correction of global simulated daily precipitation and temperature for the application of hydrological models, *Journal of Hydrology*, 395, 199 – 215, doi:<http://dx.doi.org/10.1016/j.jhydrol.2010.10.024>, <http://www.sciencedirect.com/science/article/pii/S0022169410006475>, 2010.

Raisanen, J. and Raty, O.: Projections of daily mean temperature variability in the future: cross-validation tests with ENSEMBLES regional climate simulations, *Climate Dynamics*, 41, 1553–1568, doi:[10.1007/s00382-012-1515-9](https://doi.org/10.1007/s00382-012-1515-9), <http://dx.doi.org/10.1007/s00382-012-1515-9>, 2013.



585 Raty, O., Raisanen, J., and Ylhaisi, J. S.: Evaluation of delta change and bias correction methods for future
daily precipitation: intermodel cross-validation using ENSEMBLES simulations, *Climate Dynamics*, 42,
2287–2303, doi:10.1007/s00382-014-2130-8, <http://dx.doi.org/10.1007/s00382-014-2130-8>, 2014.

Richards, L. A.: Capillary conduction of liquids through porous mediums, *Journal of Applied Physics*, 1, 318–
333, <http://scitation.aip.org/content/aip/journal/jap/1/5/10.1063/1.1745010>, 1931.

590 Rodell, M., Velicogna, I., and Famiglietti, J. S.: Satellite-based estimates of groundwater depletion in India,
Nature, 460, 999–1002, <http://dx.doi.org/10.1038/nature08238>, 2009.

Sapkota, P., Bharati, L., Gurung, P., Kaushal, N., and Smakhtin, V.: Environmentally sustainable management of
water demands under changing climate conditions in the Upper Ganges Basin, India, *Hydrological Processes*,
27, 2197–2208, doi:10.1002/hyp.9852, <http://dx.doi.org/10.1002/hyp.9852>, 2013.

595 Scoccimarro, E., Gualdi, S., Bellucci, A., Zampieri, M., and Navarra, A.: Heavy Precipitation Events in a
Warmer Climate: Results from CMIP5 Models, *J. Climate*, 26, 7902–7911, doi:10.1175/JCLI-D-12-00850.1,
<http://dx.doi.org/10.1175/JCLI-D-12-00850.1>, 2013.

Scott, C. A., S. B.: Energy supply and the expansion of groundwater irrigation in the Indus–Ganges Basin, *Int.
J. River Basin Manage.*, doi:10.1080/15715124.2009.9635374, 2009.

600 Sengupta, A. and Rajeevan, M.: Uncertainty quantification and reliability analysis of CMIP5 projections for the
Indian summer monsoon, *Current Science*, 105, 2013.

Sheffield, J., Goteti, G., and Wood, E.: Development of a 50-Year High-Resolution Global Dataset of Meteorological
Forcings for Land Surface Modeling, *Journal of Climate*, 19, 2006.

Singh, D., Horton, D., Tsiang, M., et al.: Severe precipitation in Northern India in June 2013: Causes, historical
605 context, and changes in probability [in "Explaining Extremes of 2013 from a Climate Perspective"], *Bull.
Amer. Meteor. Soc.*, 95 (9), S58–S61, 2014.

Taylor, K. E.: Summarizing multiple aspects of model performance in a single diagram, *Journal of Geophysical Research: Atmospheres*, 106, 7183–7192, doi:10.1029/2000JD900719, <http://dx.doi.org/10.1029/2000JD900719>, 2001.

610 Tenhunen, S. and Saavalta, M.: *An Introduction to Changing India: Culture, Politics and Development*, Anthem
Press, 2012.

Teutschbein, C. and Seibert, J.: Bias correction of regional climate model simulations for hydrological climate-
change impact studies: Review and evaluation of different methods, *Journal of Hydrology*, 456–457, 12
– 29, doi:<http://dx.doi.org/10.1016/j.jhydrol.2012.05.052>, <http://www.sciencedirect.com/science/article/pii/S0022169412004556>, 2012.

615 Tsarouchi, G., Mijic, A., Moulds, S., and Buytaert, W.: Historical and future land-cover changes
in the Upper Ganges basin of India, *International Journal of Remote Sensing*, 35, 3150–3176,
doi:10.1080/01431161.2014.903352, <http://dx.doi.org/10.1080/01431161.2014.903352>, 2014.

Turner, A. G.: The Indian Monsoon in a Changing Climate, *Online, Royal Meteorological Society*, <http://www.rmets.org/weather-and-climate/climate/indian-monsoon-changing-climate>, 2013.

620 Turner, A. G. and Annamalai, H.: Climate change and the South Asian summer monsoon, *Nature Clim. Change*,
2, 587–595, 2012.



Turner, A. G. and Slingo, J. M.: Uncertainties in future projections of extreme precipitation in the Indian monsoon region, *Atmospheric Science Letters*, 10, 152–158, doi:10.1002/asl.223, <http://dx.doi.org/10.1002/asl.223>, 2009.

625 van Genuchten, M. T.: A Closed-form Equation for Predicting the Hydraulic Conductivity of Unsaturated Soils, *Soil Sci. Soc. Am. J.*, 44, 892–898, 1980.

Verghese, B. G.: Harnessing the Eastern Himalayan Rivers : Regional Cooperation In South Asia, Konark Publishers Pvt. Ltd, Delhi, 1993.

630 World Bank: Turn Down The Heat: Climate Extremes, Regional Impacts and the Case for Resilience, A Report for the World Bank by the Potsdam Institute for Climate Impact Research and Climate Analytics, 2013.

Zaisheng, H., Hao, W., and Rui, C.: Transboundary Aquifers in Asia with Special Emphasis to China, United Nations Educational, Scientific and Cultural Organization, pp. 10–18, 2006.